ISBN: 978-3-95450-192-2 doi:10.18429/JACoW-IBIC2017-WEPWC10

Content from this work may be used under the terms of the CC BY 3.0 licence (© 2018). Any distribution of this work must maintain attribution to the author(s), title of the work, publisher, and DOI.

BEAM LOSS MONITORING SYSTEM FOR THE RARE ISOTOPE SCIENCE PROJECT*

Yoolim Cheon, Changkyu Sung, Kookjin Moon,
Chulun Choi, Dongnyung Choe, Moses Chung[†], UNIST, Ulsan 44919, Korea
Yeonsei Chung[‡], Gidong Kim, Hyung Joo Woo, IBS, Daejeon 34047, Korea
Chanmi Kim, Korea University, Sejong 30019, Korea

Abstract

A heavy ion accelerator facility called RAON is being constructed in Korea to produce various rare isotopes for the Rare Isotope Science Project (RISP). This facility is designed to use both In-flight Fragment (IF) and Isotope Separation On-Line (ISOL) techniques in order to provide a wide variety of RI beams for nuclear physics experiments. One of the biggest challenges in operating such a high beam power facility (~400 kW) is to monitor beam loss accurately and to execute the machine protection system reasonably quickly whenever necessary. In this work, we report the conceptual design of the RAON beam loss monitoring system. Monte Carlo simulations using MCNPX code have been performed to generate radiation dose maps for 1 W/m losses of proton and uranium beams. The required machine protection time has been estimated from the yield time of the stainless steel beam line components including the beam grazing angle dependence. Types of the detectors have been determined based on the radiation levels of the gammas and neutrons, and the minimum sensitivity and response time requirements.

INTRODUCTION

The RISP project [1] will be composed of a 70 kW proton cyclotron as a low-power ISOL driver, an 18 MeV/u linac for ISOL post-accelerator and a 200 MeV/u main linac for high-power ISOL and IFF driver. The main driver linac named RAON will accelerate all elements up to uranium with beam power up to 400 kW. To maximize the average currents of the primary beam on target, continuous wave (CW) operation is preferred, and therefore superconducting RF (SCRF) technology has been adopted for the linac design. One of the biggest challenges in operating such a high beam power facility (~400 kW) is to monitor beam loss accurately and to execute the machine protection system (MPS) reasonably quickly whenever necessary.

The role of the dedicated beam loss monitors (BLMs) includes 1) to protect beam line components from fast or irregular beam losses, 2) to minimize activation of the components for maintenance, and 3) to provide information for beam tuning and optimization. The BLM should provide the amount of beam loss, beam loss location, and fast interlock signal to inhibit the beam. The (preliminary) requirements of the RAON BLM system are summarized as follows:

- It should detect beam losses not only from proton beam, but also from heavier ion beams such Oxygen and uranium ion beams.
- It should have a high dynamic range to cover both slow (<1 W/m level) and fast (significant fraction of total beam power) beam losses.
- It should provide the interlock signal within $< 15\mu s$ (overall MPS time would be $< 35\mu s$).

MPS REQUIREMENTS

It has been known that the yield stress of the beam line components (copper, stainless-steel, or niobium etc.) indeed determines the maximum allowable beam injection time, which is given by [2–6]

$$T_{\max} \approx \frac{4\pi}{\sqrt{3}} \frac{\sigma_x \sigma_y}{I} \frac{\rho C_v}{\alpha E} \sigma_m \frac{1}{R_{ave}}, \quad (1)$$

where $\sigma_x(\sigma_y)$ is the rms beam radius in $x(y)$-direction, I is the beam current in pps, ρ is the mass density of the material, C_v is the specific heat, α is the coefficient of linear expansion, E is the Young's modulus, σ_m is the yield strength, and R_{ave} is the average stopping power of the Bragg curve which is estimated from the SRIM code. Because the stopping power of a heavy ion beam is a few ten times larger than proton or electron beams, a fast response of the MPS (faster than the material damage time) is even more important in heavy ion machines.

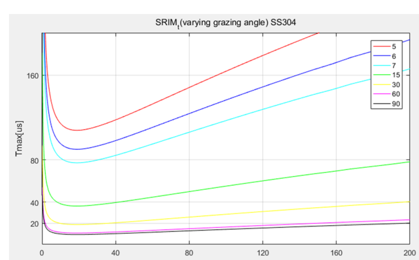

Figure 1: The maximum allowable injection time depends on the incidence angle (~2 orders of magnitude difference).

The required response time strongly depends on incident angle of the beam (θ) as well. Figure 1 shows $T_{\max}$ for the case of uranium beam injecting into stainless-steel (SS) along the RISP linac (see the linac structure in Fig. 2). For incident angles larger than 60 degrees, the damage may happen in less than 20 μs, which is beyond the capability of

* Work supported by the National Research Foundation of Korea (Grants No. NRF-2017M7A1A1019375 and No. NRF-2017M1A7A1A02016413).
† mchung@unist.ac.kr
‡ yschung@ibs.re.kr

ISBN: 978-3-95450-192-2 doi:10.18429/JACoW-IBIC2017-WEPWC10

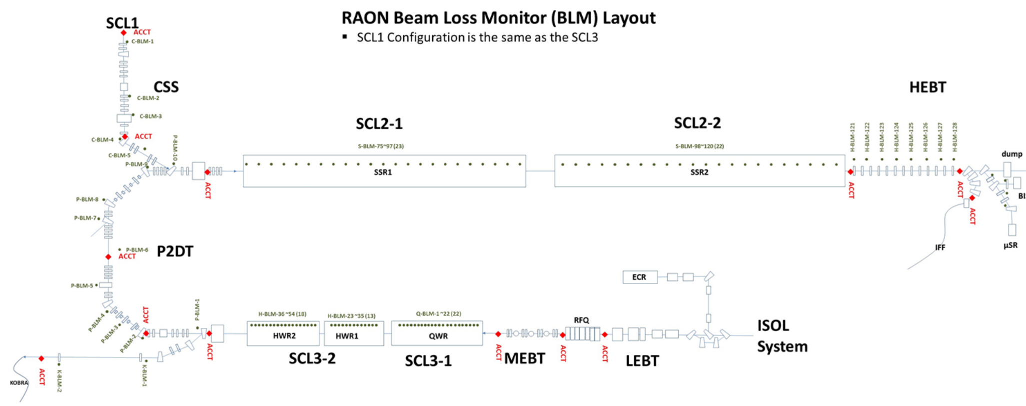

Figure 2: Layout of the RAON beam loss monitoring system. Green dots indicate BLMs while red diamonds ACCTs.

the RISP MPS. The 90 degree angle is the worst case which makes the maximum damage on the components. Nevertheless, such case can occur very rarely, for example only when objects (e.g., gate valve) are in the beam line or beam hits the bellows. In most cases, it is expected that the incident angle is small enough that the response time of $\sim 35\mu s$ would be reasonable.

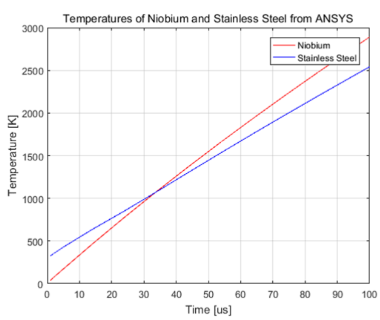

Figure 3: Thermal analysis on Nb and SS by ANSYS with uranium beam of 1-mm rms radius, Gaussian profile, and 90 degree grazing angle.

An ANSYS thermal analysis suggests that indeed the SS yield happens faster than the melting of SS and Nb (see Fig. 3). Temperature rise in a short time is mainly determined by beam deposited power density, and specific heat of the material. Melting times of SS and Nb are $\sim 46\ \mu s$ and $\sim 69\ \mu s$, respectively, which are longer than the overall MPS time requirement of $\sim 35\ \mu s$.

LAYOUT OF THE RAON BLM SYSTEM

A preliminary layout of the RAON BLM system is illustrated in Fig. 2. In the superconducting linac sections, one BLM per warm section (i.e., near the quadrupole doublet) will be installed. In the bending sections [post linac to driver linac transport (P2DT) and charge stripper section (CSS)], BLMs will be installed around the possible beam loss points, such as collimators, bending magnets, etc. Currently, total 182 BLMs are planned.

Before and after the sections where a beam transport monitoring is critical, AC-coupled current transformers (ACCTs) are planned to be installed. The signal difference by two ACCTs makes an alarm signal for machine protection. This differential beam current monitor (DBCM) networks will be used as a primary MPS input for fast beam losses.

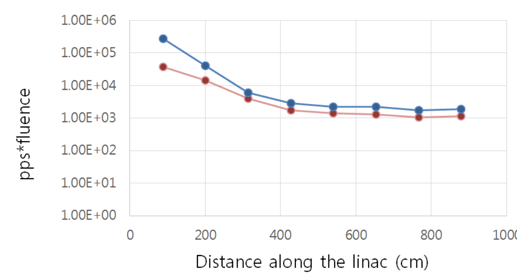

Figure 4: Neutron flux along the position of the doublets for the case of a point loss in the doublet with 3 mrad incidence angle and 1 W of total beam loss. An uranium beam of 200 MeV/u is used in this calculation. Case 1(2) corresponds to the detector position inside(outside) the doublet.

FAST LOSS SCENARIO

Due to the lack of complete list of beam loss patterns, some strategy is needed to determine the number of detectors and their locations [6]. The TRACK simulations indicate that most localized losses occur in the quadrupoles (except the slit), in which the beam size is largest. Therefore, as a default, we decided to place one BLM per one quadrupole doublets in the warm sections. To see the basic characteristics of the fast losses, we perform Monte-Carlo simulations (MCMPX) for point losses in the quadrupoles with 3 mrad incidence angle and 1 W of total beam loss. Figure 4 implies that the neutron flux is sufficiently localized that one might tell at which doublet the beam loss occurs. As a future work, we will increase the incidence angle to the "worst case angle" to do fine-tuning of the BLM locations, following ESS's approach.

Content from this work may be used under the terms of the CC BY 3.0 licence (© 2018). Any distribution of this work must maintain attribution to the author(s), title of the work, publisher, and DOI.

ISBN: 978-3-95450-192-2 doi:10.18429/JACoW-IBIC2017-WEPWC10

Content from this work may be used under the terms of the CC BY 3.0 licence (© 2018). Any distribution of this work must maintain attribution to the author(s), title of the work, publisher, and DOI.

Table 1: Beam Energy Variation along the Superconducting Linac Sections of the RAON

	QWR	HWR1	HWR2	SSR1	SSR2
Uranium	0.5~2.6 MeV/u	2.6~6 MeV/u	6~18.5 MeV/u	18~56.3 MeV/u	56.3~210.4 MeV/u
Proton	0.5~7.5 MeV/u	7.5~34.2 MeV/u	34.2~87.4 MeV/u	87.4~222 MeV/u	222~600 MeV/u

RADIATION SIMULATIONS

To estimate the radiation doses from 1 W/m level of slow losses, we carried out the MCNPX (Version 2.7.0) Monte-Carlo simulations. A line source with particle flux equivalent to 1 W/m is assumed. The incident angle is set 90 degrees. Average doses are calculated on cylindrical detectors located outside the cryomodules. The geometry inputs for the MCNPX simulations are semi-realistic, i.e., the structures themselves are made bulky without minor details, but material densities and masses are close to the real values (see Fig. 5).

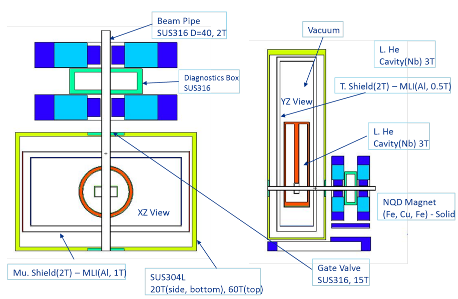

Figure 5: An example of the geometry used for the MCNPX simulations. Shown here is the QWR section.

The normalized (by 1 W/m) neutron flux (#/cm^2/s) and gamma dose (rad/hr) are shown in Figs. 6 and 7, respectively as functions of beam energy. The energy variations of the proton and uranium beams along the superconducting linacs are summarized in Table 1. We note that for a given beam energy per nucleon, radiations induced by heavy ions are much weaker than those induced by protons. We also note that the neutron generation is negligible when the beam energy is less than 10 MeV/u. From Figs. 6 and 7, we expect that beam loss monitoring for the uranium beam in the low energy linac sections would be extremely challenging.

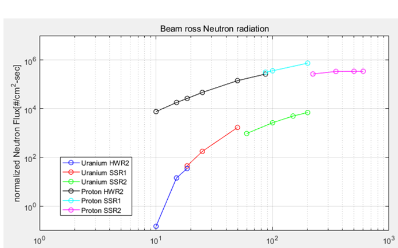

Figure 6: Neutron flux versus beam energy for 1 W/m loss.

As shown in Figs. 8 and 9, the neutron energy spectrum becomes wider as beam energy goes higher while the gamma energy spectrum has more or less a fixed range.

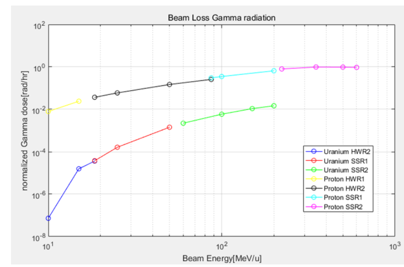

Figure 7: Gamma does versus beam energy for 1 W/m loss.

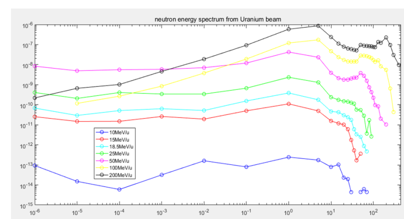

Figure 8: Neutron fluence from a single uranium beam ion.

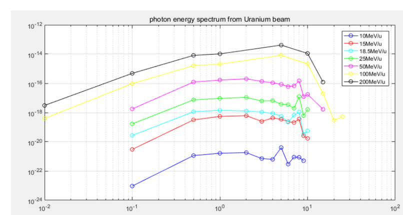

Figure 9: Gamma fluence from a single uranium beam ion.

CAVITY X-RAY ISSUES

Not only from the beam losses in the beam pipe but also from the bremsstrahlung of field-emitted electrons inside the cavity, significant photon radiation can be made. Estimation of the maximum X-ray dose for each linac section is summarized in Table 2. This cavity X-ray indeed acts as a background noise for the BLM detectors, and can exceed the beam loss signal particularly for heavy ions in the low energy sections [7, 8]. As shown in Fig. 10, most X-ray energy lies below 1 MeV for low energy linacs. Therefore, we may use lead to shield low energy photons (< 1 MeV) to separate gamma radiation generated by the beam loss from the cavity X-ray background.

BLM DETECTORS

For low energy, we consider plastic detectors (PD, plastic scintillators + PMTs) because they are fast and have high efficiency for fast neutrons and high energy gamma rays [9–11]. For higher energies, ionization chambers (IC), which almost all accelerators in the world are equipped with, will

ISBN: 978-3-95450-192-2 doi:10.18429/JACoW-IBIC2017-WEPWC10

Table 2: Estimation of the Maximum X-ray Dose for each Linac Section

	QWR	HWR1	HWR2	SSR1	SSR2
Accelerating voltage (MV)	1.1	1.4	1.4	2.3	4.1
Maximum head load (W)	1.6	2.7	2.7	4.5	8
Maximum field emission flux (#/sec)	9.1E+12	1.2E+13	1.2E+13	1.2E+13	1.2E+13
Maximum dose (rad/hr)	3.75E-02	4.97E-02	4.97E-02	5.04E-02	5.03E-02

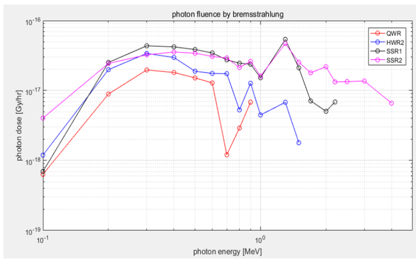

Figure 10: Cavity X-ray energy spectrum.

Table 3: Target Radiation and Particle Species for each BLM Detector

	IC	PD	HRD	ACCT
QWR	N/A	N/A	Beam ions	EM fields
HWR1	N/A	γ	Beam ions	EM fields
HWR2	N/A	γ, n	Beam ions	EM fields
SSR1	γ	γ, n	Beam ions	EM fields
SSR2	γ	γ, n	Beam ions	EM fields

be a better solution in terms of cost and maintenance. The strategy for the RAON BLM systems is summarized in Table 3. For low energy sections (QWR and HWRs), beam loss monitoring by secondaries will be very difficult, thus an interceptive device called Halo Ring Detector (HRD) [7, 8] is also under preparation.

For the scintillator material, we consider BC-408 (or EJ-200). This organic plastic is less sensitive to low energy X-ray, and interacts with fast neutrons (>50 keV) through (n,p) scattering. For 1000 g of BC-408, the sensitivity of the scintillation detector is [9, 10]

$$S_{scint} \approx 140 \left[\frac{\mathrm{C}}{\mathrm{rad}}\right] \times \varepsilon_{coll}, \tag{2}$$

where ε_{coll} is the efficiency of collector or light guide. Here, we assume the light output $R_s = 0.1$ photon/eV and the PMT gain is 7×10^5. The detection efficiency of BC-408 to fast neutrons can be calculated based on np-scattering cross-section for 5 cm-long BC-408 plastic scintillator, which is parameterized as [12]

$$DE = -0.142 \ln(E_n) + 0.5247, \tag{3}$$

where E_n is the neutron energy in MeV. For 1 liter (1000 cm^3) argon filled ionization chamber at 1 atm, the sensitivity is [9, 10]

$$S_{ion} \approx 638 \left[\frac{\mathrm{nC}}{\mathrm{rad}}\right]. \tag{4}$$

Coupled with radiation simulations, we can estimate the actual signal levels of IC, PD, and HRD in each linac section, which is in progress and will be reported elsewhere. Design and fabrication of the prototype detectors are also underway (see Fig. 11).

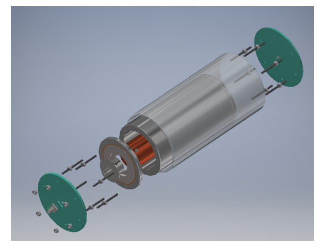

Figure 11: Preliminary 3D drawing of the coaxial ionization chamber.

REFERENCES

[1] RISP web page, http://www.risp.re.kr.

[2] R. E. Shafer, "How Long a SNS Beam Pulse Would Damage a Copper Accelerating Structure?", SNS Technical Note (2001).

[3] C. Sibley, "Machine Protection Stratiges for High Power Accelerators", *Proceedings of the 2013 Particle Accelerator Conference*, Portland, Oregon, USA (2003).

[4] H. Takei *et al.*, *Journal of NUCLEAR SCIENCE and TECHNOLOGY*, Vol. 42, No. 12, p. 1032–1039 (December 2005).

[5] Y. Zhang *et al.*, "Analysis of Beam Damage to FRIB Driver Linac", *Proceedings of SRF2011*, Chicago, IL, USA (2011).

[6] I. Dolenc Kittelmann *et al.*, "Simulations and Detector Technologies for the Beam Loss Monitoring System at the ESS Linac", *Proceedings of HB2016*, Malmö, Sweden (2016).

[7] Z. Liu *et al.*, "Beam Loss Monitor System for the Low-Energy Heavy-Ion FRIB Accelerator", *Proceedings of IBIC2013*, Oxford, UK (2013).

[8] Z. Liu *et al.*, "Collimation Design and Beam Loss Detection at FRIB", *Proceedings of HB2016*, Malmö, Sweden (2016).

[9] K. Wittenburg, "Beam Loss Monitors", CAS2008: Specialised Beam Diagnostics School, Dourdan, France (2008).

[10] K. Wittenburg, "Beam Loss Monitors: Overview of BLM Technology", 3rd oPAC Topical Workshop on Beam Diagnostics, Vienna (2014).

[11] F. Negoita, Private Communications (2017).

[12] J. Va'vra *et al.*,"Neutron Beam Line at SLAC", SLAC-TN-14-026 (2014).

Content from this work may be used under the terms of the CC BY 3.0 licence (© 2018). Any distribution of this work must maintain attribution to the author(s), title of the work, publisher, and DOI.